The Temporal Response of the Length of a Partially Stratified Estuary to Changes in River Flow and Tidal Amplitude

JAMES A. LERCZAK

College of Oceanic and Atmospheric Sciences, Oregon State University, Corvallis, Oregon

W. ROCKWELL GEYER AND DAVID K. RALSTON

Woods Hole Oceanographic Institution, Woods Hole, Massachusetts

(Manuscript received 19 October 2007, in final form 17 September 2008)

ABSTRACT

The temporal response of the length of a partially mixed estuary to changes in freshwater discharge Q_f and tidal amplitude U_T is studied using a 108-day time series collected along the length of the Hudson River estuary in the spring and summer of 2004 and a long-term (13.4 yr) record of Q_f, U_T, and near-surface salinity. When Q_f was moderately high, the tidally averaged length of the estuary L_5, here defined as the distance from the mouth to the up-estuary location where the vertically averaged salinity is 5 psu, fluctuated by more than 47 km over the spring–neap cycle, ranging from 28 to >75 km. During low flow periods, L_5 varied very little over the spring–neap cycle and approached a steady length. The response is quantified and compared to predictions of a linearized model derived from the global estuarine salt balance. The model is forced by fluctuations in Q_f and U_T relative to average discharge Q_o and tidal amplitude U_{To} and predicts the linear response time scale τ and the steady-state length L_o for average forcing. Two vertical mixing schemes are considered, in which 1) mixing is proportional to U_T and 2) dependence of mixing on stratification is also parameterized. Based on least squares fits between L_5 and estuary length predicted by the model, estimated τ varied by an order of magnitude from a period of high average discharge ($Q_o = 750$ m^3 s^{-1}, $\tau = 4.2$ days) to a period of low discharge ($Q_o = 170$ m^3 s^{-1}, $\tau = 40.4$ days). Over the range of observed discharge, $L_o \propto Q_o^{-0.30\pm0.03}$, consistent with the theoretical scaling for an estuary whose landward salt flux is driven by vertical estuarine exchange circulation. Estimated τ was proportional to the discharge advection time scale (L_oA/Q_o, where A is the cross-sectional area of the estuary). However, τ was 3–4 times larger than the theoretical prediction. The model with stratification-dependent mixing predicted variations in L_5 with higher skill than the model with mixing proportional to U_T. This model provides insight into the time-dependent response of a partially stratified estuary to changes in forcing and explains the strong dependence of the amplitude of the spring–neap response on freshwater discharge. However, the utility of the linear model is limited because it assumes a uniform channel, and because the underlying dynamics are nonlinear, and the forcing Q_f and U_T can undergo large amplitude variations. River discharge, in particular, can vary by over an order of magnitude over time scales comparable to or shorter than the response time scale of the estuary.

1. Introduction

Tidally averaged, physical conditions of an estuary—including the length of the salinity intrusion, the strength of stratification, and the strength and structure of the subtidal estuarine exchange circulation—are set by competing external forcing mechanisms. In many partially mixed estuaries, the dominant forcing mechanisms are buoyancy forcing by river discharge Q_f and stirring and mixing due to tidal currents. For steady discharge and tidal amplitude, estuary length, exchange circulation, and stratification tend toward steady values. For time-varying forcing, the estuary adjusts as it is driven toward a new equilibrium set by instantaneous forcing conditions. In partially stratified estuaries, for example, a reduction in tidal amplitude and associated tidally generated mixing and vertical shear stress causes available potential energy (APE), associated with tilted isopycnals and the longitudinal density gradient, to be released, initially causing the exchange circulation to

Corresponding author address: James A. Lerczak, College of Oceanic and Atmospheric Sciences, Oregon State University, 104 COAS Administration Building, Corvallis, OR 97331-5503.
E-mail: jlerczak@coas.oregonstate.edu

DOI: 10.1175/2008JPO3933.1

accelerate and stratification to increase. The length of the estuary increases as the salinity intrusion slumps landward and the longitudinal density gradient decreases toward a new equilibrium. With an increase in tidally generated mixing, the exchange circulation decelerates, stratification is reduced, and river discharge advects the salinity intrusion oceanward, thereby reducing the length of the estuary.

River discharge provides the buoyancy that maintains stratification and the longitudinal salt gradient. An increase in river discharge, for example, increases stratification and increases APE of the estuary by reducing its length and increasing its longitudinal salt gradient.

The amplitude and timing of the response of an estuary to time variations in forcing is dependent on the sensitivity of the estuary to the forcing and the intrinsic time scale by which the estuary responds to changes compared to the time scales over which the forcing varies (Kranenburg 1986; Hetland and Geyer 2004; MacCready 2007). If the response time τ is much shorter than the time scale of variations in forcing, the estuary will remain in a quasi–steady state relative to instantaneous forcing conditions (Hetland and Geyer 2004; MacCready 2007). If τ is comparable to or longer than the time scale of forcing variations, the estuary cannot keep pace with forcing variations and the estuary remains in an unsteady, time-dependent state (Vallino and Hopkinson 1998; Simpson et al. 2001; Banas et al. 2004; Lerczak et al. 2006). The estuary response time depends not only on the underlying nonlinear dynamics that regulate the salt balance within an estuary but also on the mean forcing about which the variations occur and the background state of the estuary itself (Kranenburg 1986; Smith 1996; MacCready 2007).

Here, we study the response of the length of the Hudson River estuary to changes in tidal amplitude and river discharge, using a 108-day time series of salinity and current measurements collected along the length of the salinity intrusion in the spring and summer of 2004 and a long-term (13.4 yr) record of Q_f, U_T, and near-surface salinity. The Hudson River estuary, a partially mixed estuary that drains into the mid-Atlantic Bight off of northeast United States (Fig. 1), undergoes large variations in structure on various time scales including the spring–neap cycle, storm-event scales, and seasonal scales (Abood 1974; Wells and Young 1992; Geyer et al. 2000; Bowen and Geyer 2003; Geyer and Chant 2006). For spring freshet conditions, Q_f can exceed 4000 $m^3 s^{-1}$ and the length of the salinity intrusion is typically <30 km. During low discharge periods typical of late summer and early fall ($Q_f < 200$ $m^3 s^{-1}$), the length of the salinity intrusion can exceed 100 km.

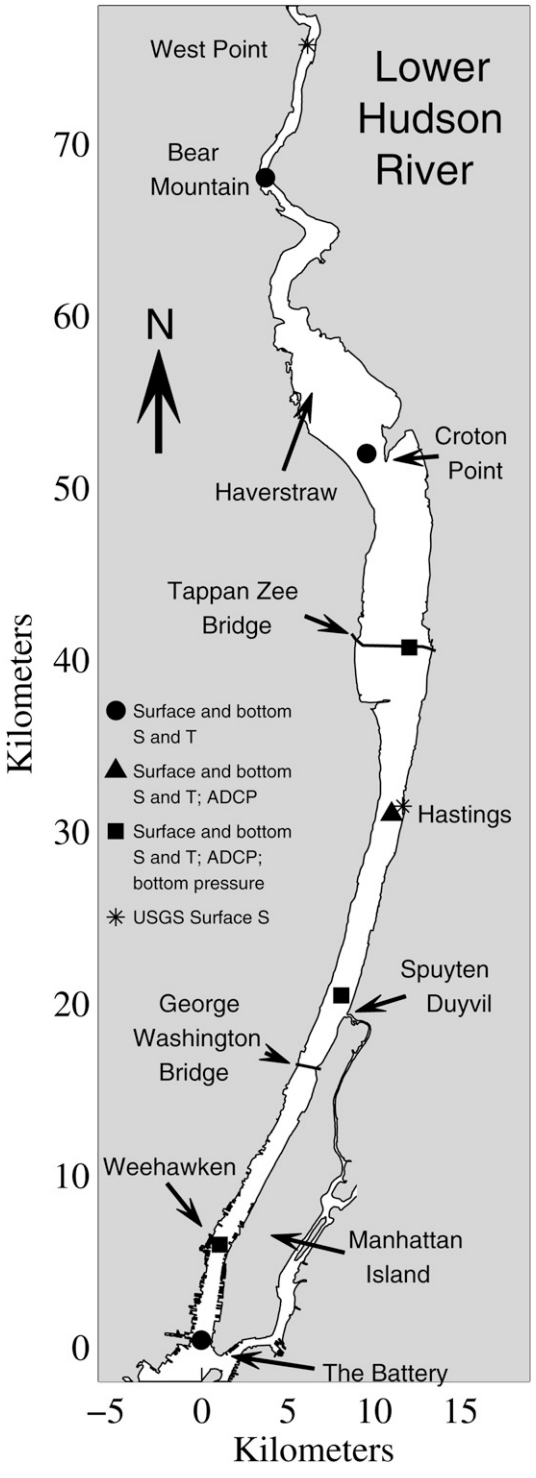

FIG. 1. Map of the Hudson River estuary showing the locations of the moorings deployed along the estuary during the spring and summer of 2004 and locations of long-term time series. Locations of the USGS near-surface salinity time series at Poughkeepsie (120 river km from the Battery) and the USGS stream gauge time series at the Green Island Dam (~250 river km from the Battery) are not shown.

Several observational studies have shown that, under most conditions, the salt balance within the estuary is not in a steady state with respect to instantaneous forcing conditions (Bowen and Geyer 2003; Lerczak et al. 2006). Using data from several studies spanning 40 yr, Abood (1974) observed that the length of the Hudson salinity intrusion was proportional to $Q_f^{-1/3}$ for low to moderately high discharge ($Q_f < 1000$ m^3 s^{-1}), consistent with the scaling predicted by the steady-state theory of Hansen and Rattray (1965) (Monismith et al. 2002). For higher discharge, the estuary length was observed to be more sensitive to changes in Q_f. Abood (1974) suggests that the response of the salinity intrusion lags changes in Q_f by 5–10 days, with the lag time decreasing with increasing Q_f. Bowen and Geyer (2003) report on the length of the estuary changing very little with spring–neap changes in tidal amplitude during a persistent period of low Q_f and then decreasing rapidly in response to a high discharge event.

The adjustment of the Hudson estuary to changes in forcing has also been described in several modeling studies (Warner et al. 2005; MacCready 2007; Ralston et al. 2008). MacCready (2007) developed a tidally and cross-sectionally averaged numerical model—based on the quasi-steady theory of Hansen and Rattray (1965) and Chatwin (1976) for estuarine exchange circulation, salinity stratification, and the volume-integrated salt balance—in order to study the dependence of the structure of the salinity intrusion on changes in river discharge and tidal mixing. When applied to the Hudson estuary, the model predicts a response time that is strongly dependent on mean river discharge (e.g., $\tau = 3$ and 31 days for a mean Q_f of 1000 and 100 m^3 s^{-1}, respectively). Ralston et al. (2008) used a numerical model based on MacCready (2007), modified to include wind forcing and sea level variability at the open boundary and using a different vertical mixing scheme than that used by MacCready (2007), in order to assess the model's skill in predicting variations in stratification, vertical exchange circulation and estuary length as observed in the Hudson estuary in 2004, using the same dataset used in this study. In addition, they observed that, for fixed tidal amplitude and constant river discharge, the model predicts a steady-state length that varies with discharge according to $Q_f^{-0.35}$, consistent with Abood (1974).

These observational and modeling studies are all consistent with the response time of the Hudson being strongly dependent on river discharge. However, the response time and its dependence on mean forcing conditions has not yet been quantified based on observations. Quantifying the response time from observations is challenging because it requires time series of vertically averaged salinity at multiple locations along an estuary in order to effectively estimate variations in estuary length. Time series must also be sufficiently long in order to resolve variations in length over a broad range of forcing conditions.

The three main objectives of this analysis are to 1) quantify the linear response time of estuary length and its dependence on mean river discharge, based on long-term observations in the Hudson, and compare it to theoretically derived response times; 2) determine the sensitivity of response (linear response amplitude relative to forcing amplitude) to spring–neap variations in tidal amplitude and its dependence on mean river discharge; and 3) quantify the scaling relationship between equilibrium estuary length and mean river discharge and compare this to theoretical scalings derived from a steady-state estuary model. We accomplish these objectives by fitting the observed length of the estuary to a linear model describing temporal variations in estuary length caused by variations in river discharge and tidal amplitude.

The remainder of the manuscript is organized as follows. The linear response model is developed in section 2, where two vertical mixing schemes are considered: 1) vertical eddy viscosity and diffusivity are proportional to tidal amplitude and 2) mixing is parameterized to take into account the influence of stratification. The data used in this analysis are described in section 3 and the method for fitting the data to the model is described in section 4. In section 5, derived estuary response parameters and their dependence on background river discharge are summarized. Finally, the results from this study are discussed and generalized in sections 6 and 7.

2. Linear response model derived from estuarine salt balance

We adopt the approach of Kranenburg (1986) and MacCready (2007) and consider the response of the salt balance within an estuary to infinitesimal changes in freshwater discharge and vertical mixing. The derivation of the linear response model is essentially the same as that of MacCready (2007). Our development of the model expands beyond that of MacCready (2007) by considering the effects of a stratification-dependent vertical mixing scheme and by considering a general form for the along-estuary salt dispersion rate (see section 6d).

The subtidal, longitudinal salt balance can be expressed as an advection–diffusion equation as follows (Harleman and Thatcher 1974; Kranenburg 1986; Monismith et al. 2002):

$$A\frac{\partial}{\partial t}S = \frac{\partial}{\partial x}\left(Q_f S + AK\frac{\partial S}{\partial x}\right), \tag{1}$$

where S is the subtidal, cross-sectionally averaged salinity at some location along the estuary; A is the cross-sectional area of the estuary; x is the along-estuary distance increasing in the upstream direction; and K is the along-estuary salt dispersion rate. The up-estuary salt flux, expressed in Fickian form [last term in Eq. (1)], includes all processes that contribute to this flux. In the central portion of the Hudson estuary, this flux is dominated by steady shear dispersion due to the subtidal, estuarine exchange circulation acting on a stratified salt field (Hunkins 1981; Bowen and Geyer 2003; Lerczak et al. 2006). In the idealized, steady-state estuarine model of Hansen and Rattray (1965), the dispersion rate due to estuarine exchange is expressed as (Chatwin 1976)

$$K = \alpha\frac{(g\beta)^2 H^8}{\kappa\nu^2}\left|\frac{\partial S}{\partial x}\right|^2, \tag{2}$$

where α is a constant ($\approx 1.3 \times 10^{-5}$), g is the gravitational acceleration, β is the coefficient of saline expansion, H is the water depth, and κ and ν are depth-independent vertical eddy diffusivity and viscosity, respectively.

MacCready (2007) and Ralston et al. (2008) solve Eq. (1) to study variations in the salinity intrusion to changes in forcing, and include along-estuary variations in depth and cross-sectional area. In addition to the dispersion rate expressed in Eq. (2), they include an along-estuary tidal dispersion term. However, when applied to the Hudson, tidal dispersion, as parameterized in the model, decreases rapidly beyond one tidal excursion from the estuary mouth. Estuarine exchange is the dominant dispersion mechanism, except, perhaps, when discharge is very high and the length of the estuary approaches a tidal excursion in length. In the derivation of the linear response model below, we do not include tidal dispersion and we assume a uniform estuarine channel.

We consider an idealized estuarine salinity distribution in which S reduces linearly from S_o at the ocean end of the estuary ($x = 0$) to zero a distance L up the estuary (Fig. 2). Integrating (1) over the full length of the estuary, with (2) used for the dispersion rate, gives an expression for the time rate of change of the length of the estuary:

$$\frac{1}{2}AS_o\frac{dL}{dt} = -Q_f S_o + \alpha\frac{(g\beta)^2 H^8}{\kappa^3}A\frac{S_o^3}{L^3}. \tag{3}$$

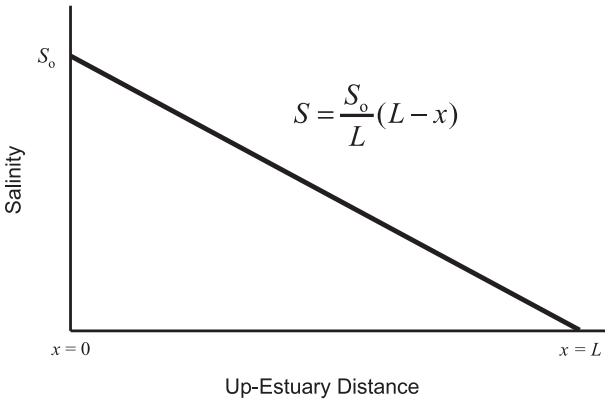

FIG. 2. Idealized cross-sectionally averaged salinity vs distance along an estuary. Here S_o is the salinity at the ocean end of the estuary and L is the length of the estuary.

For simplicity, we assume a turbulent Schmidt number, the ratio of eddy viscosity to eddy diffusivity, of one ($\nu = \kappa$).

a. Vertical mixing scheme

Two parameterizations for vertical mixing are considered. In the first, we assume that the tidal amplitude sets the velocity scale for eddies and the water depth sets the eddy length scale, giving an eddy diffusivity of

$$\kappa = a_o C_d U_T H, \tag{4}$$

where a_o is a constant, C_d is the quadratic drag coefficient, and U_T is the tidal current amplitude. This parameterization accounts for the dependence of bottom-boundary-generated vertical mixing on tidal amplitude. However, it does not account for the suppression of mixing due to stratification, which has been recognized to influence estuarine response (Monismith et al. 2002; MacCready 2007; Ralston et al. 2008). For example, Monismith et al. (2002) suggest that the weak dependence of the length of the northern San Francisco Bay estuary on river discharge is due to enhanced stratification and consequent suppression of vertical mixing with increasing river discharge.

Ralston et al. (2008) parameterize the stratification dependence of vertical mixing by scaling the eddy viscosity and diffusivity with the thickness of the bottom-boundary layer h_{bl} rather than the depth of the water column H:

$$\kappa = b_o C_d U_T h_{\mathrm{bl}}, \tag{5}$$

where b_o is a constant. The scale for the boundary layer thickness is obtained by assuming that the production of stratification due to straining of dS/dx is balanced by

mixing at the top of the boundary layer (Stacey and Ralston 2005):

$$h_{bl} = H\left(\frac{R_{fc}}{\mathrm{Ri}_x}\right)^{1/2}, \tag{6}$$

where R_{fc} is a constant critical flux Richardson number and Ri_x is the horizontal Richardson number; $\mathrm{Ri}_x = -g\beta H^2(dS/dx)/(C_d U_T)^2$ (Stacey et al. 2001). With this formulation, eddy diffusivity scales with ${U_T}^2$ and with $(dS/dx)^{-1/2}$.

b. Linearized estuary response

Linearizing (3) about infinitesimal changes in freshwater discharge (Q'), tidal amplitude (U_T'), and estuary length (L') about equilibrium values (Q_o, U_{To}, and L_o, respectively), gives the following linear response equation:

$$\frac{dL'}{dt} + \frac{1}{\tau}L' = \frac{L_o}{\tau}f(t), \tag{7}$$

where τ is the linear response time and f is a forcing function dependent on fluctuations in river discharge and tidal amplitude. Equation (3) could also be linearized about changes in cross-sectionally averaged salinity at the ocean end of the estuary S_o. However, we choose not to do so, because temporal variations in S_o are small (12% variations about average S_o in 2004; see section 3a) compared to temporal variations in U_T (~50% variations about the mean) and Q_f (fluctuations greater than an order of magnitude in amplitude).

For the two mixing schemes described above, f, L_o, and τ are

$$\begin{aligned} f_1 &= -\left(\frac{1}{3}\frac{Q'}{Q_o} + \frac{U_T'}{U_{To}}\right), \\ f_2 &= -\frac{4}{3}\left(\frac{1}{6}\frac{Q'}{Q_o} + \frac{U_T'}{U_{To}}\right); \end{aligned} \tag{8}$$

$$\begin{aligned} L_{o1} &= \left[\alpha\frac{(g\beta S_o)^2 H^5 A}{(a_o C_d)^3}\right]^{1/3}\frac{1}{U_{To}Q_o^{1/3}}, \\ L_{o2}, &= \left[\frac{\alpha(g\beta S_o)^{7/2}\, H^8 A}{b_o^3 C_d^{9/2}}\right]^{2/9}\frac{1}{U_{To}^{4/3}Q_o^{2/9}}; \quad \text{and} \end{aligned} \tag{9}$$

$$\tau_1 = \frac{L_o A}{6Q_o}, \qquad \tau_2 = \frac{L_o A}{9Q_o}. \tag{10}$$

In the model with vertical mixing proportional to tidal amplitude, referred to with subscript 1, the equilibrium length of the estuary is proportional to ${U_{To}}^{-1}$ and ${Q_o}^{-1/3}$ (Monismith et al. 2002; Hetland and Geyer 2004). Consequently, the response of the estuary is more sensitive to changes in tidal amplitude compared to changes in discharge, as reflected by the factor of one-third that multiplies the discharge variations in the forcing term [bracketed expression of Eq. (8)]. The estuary response time is predicted to be one-sixth the time it takes a water parcel, traveling at the speed of the freshwater discharge (Q_o/A), to traverse the length of the estuary (Kranenburg 1986; Hetland and Geyer 2004; MacCready 2007).

When stratification dependence is included in the mixing scheme (referred to with subscript 2), the strength of forcing due to tidal amplitude fluctuations increases, relative to river discharge forcing, as is apparent in Eq. (8). The equilibrium length has a stronger dependence on the background tidal amplitude and a weaker dependence on river discharge. In addition, the response time is predicted to be shorter for a particular river discharge.

c. Response to sinusoidally varying forcing

The solution to (7) for sinusoidally varying forcing, $f \equiv a\sin(\omega t)$, is

$$L = L_o\left[1 - \frac{a}{\sqrt{1+\omega^2\tau^2}}\sin(\omega t - \varphi)\right] + \Delta e^{-t/\tau}, \tag{11}$$

where $\varphi = \arctan(\omega\tau)$ and Δ is the amplitude of an initial transient that decays at the response time scale. For response times much smaller than the forcing period ($\tau/T_f = \omega\tau/2\pi \ll 1$), the response amplitude of L for a given forcing amplitude a is maximal; L' is nearly in phase with the forcing; and the estuary is in a quasi-steady balance with respect to instantaneous forcing conditions (Fig. 3) after the initial transient decays. As the response time increases, the amplitude of L' decreases and lags the forcing, with the phase lag approaching 90° for very long response times. Even for response times comparable to the forcing period ($\tau/T_f \approx 1$), the response of the estuary is significantly muted (Fig. 3), and the estuary is not in a quasi–steady state; that is, the tendency term in (7) is a significant term in the balance.

For the Hudson, with river discharge that ranges from about 100–4000 $\mathrm{m^3\ s^{-1}}$, a cross-sectional area of approximately $1.5 \times 10^4\ \mathrm{m^2}$, and a typical length of about 50 km, the predicted linear response time τ_1 ranges from 0.4 to 15 days from high discharge to low discharge conditions. Therefore, variations in the length of the estuary due to spring–neap variations in vertical mixing ($T_f \approx 14.8$ days) are predicted to be large during periods of high discharge ($\tau \ll T_f$) and

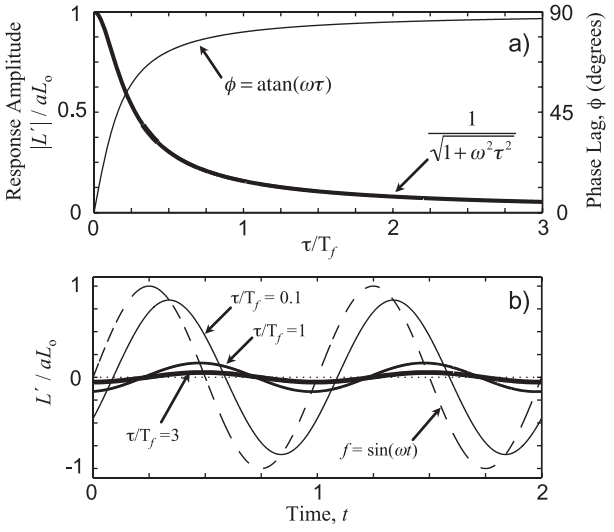

FIG. 3. (a) Nondimensional response amplitude of estuarine length (thick line) vs nondimensional response time. Amplitude is scaled by maximum response to sinusoidally varying forcing (aL_o). Response time is scaled by forcing period. Response phase lag (thin line) vs nondimensional forcing period. (b) Nondimensional, sinusoidal variations in estuary length vs time for three different estuarine response times. The forcing function f is indicated by a dashed line.

minimal during periods of low discharge ($\tau \geq T_f$, Fig. 3).

3. Description of data and processing

a. 2004 field study

Measurements of temperature, conductivity, current velocity, and bottom pressure were collected at seven locations along the lower Hudson River (Fig. 1), spanning an along-river distance of 75 km, for a period of 108 days from 24 March to 11 July 2004. At each location, temperature and conductivity were measured about 1 m below the surface from instruments attached to either surface moorings or pier pilings. Temperature and conductivity were also measured about 0.7 m from the bottom using sensors attached to bottom tripods at the thalweg of the channel at the seven locations. Pressure sensors and acoustic Doppler current profilers were also attached to some of the tripods (Fig. 1). All instruments recorded good data for the duration of the study, except for the surface sensors at the Battery, where we estimated the surface salinity based on surface salinity at the adjacent station and the bottom salinity gradient between the two stations. Detailed descriptions of the time-varying stratification, exchange circulation, and longitudinal salinity gradient can be found in Ralston et al. (2008).

In addition to the moored time series, along-estuary hydrographic surveys were conducted on the day after mooring deployment and the four days preceding recovery. The surveys spanned the length of the salinity intrusion, from the Battery to the up-river location where the salinity was less than 1 psu.

The amplitude of semidiurnal tidal currents U_T at Spuyten Duyvil (Fig. 1) was estimated by first calculating a tidal harmonic fit u_T to the vertically averaged along-channel current time series measured by the ADCP at that location and including all significant tidal constituents. Here U_T was estimated as the amplitude of a running harmonic fit to u_T for just the M_2 semidiurnal constituent using a running time block two semidiurnal periods in length (24.84 h). This allowed for spring–neap variations in U_T to be resolved. Over the 108 days of the field study, U_T ranged from 0.45 to 1.0 m s^{-1}, with seven spring tides and eight neap tides occurring over the study period (Fig. 4b).

Two storms occurred, centered on days 94 and 148, with peak oceanward freshwater fluxes of 3200 and 2100 m^3 s^{-1}, respectively (Fig. 4a; from the ADCP records). Generally, Q_f was strong before day 160 and was weak thereafter. Between days 113 and 135, Q_f was nearly steady, with an average value of 750 m^3 s^{-1}. After day 165, average Q_f was 170 m^3 s^{-1}. The average of the surface and bottom subtidal salinity at the ocean end of the estuary S_o increased roughly linearly from 18 to 23 psu (Fig. 4c).

To estimate the tidally averaged length of the estuary, we first estimated the vertically averaged subtidal salinity at the seven locations along the estuary by averaging the surface and bottom subtidal salinity at each location, and then linearly interpolated these averages between locations to determine the along-estuary location of a particular low salinity value. The time-varying along-estuary locations of the 1-, 2-, and 5-psu salinity values (L_1, L_2, and L_5, respectively) are shown in Fig. 4d.

The three lengths, L_1, L_2, and L_5, are highly correlated throughout the entire record. On average, the difference between L_5 and L_2 was 13 km and the difference between L_5 and L_1 was 19 km. However, after day 165, a low-gradient tail developed at the landward end of the estuary during the low flow conditions and the separation between L_5 and L_2 exceeded 20 km, and L_1 and L_2 extended beyond the range of the mooring array. Similar to the findings of Monismith et al. (2002) for northern San Francisco Bay, the along-estuary structure of S in the Hudson is nearly self-similar when S is scaled by S_o and x is scaled by L_5 (Fig. 5). The salinity gradient is roughly linear over most of the extent of the salinity intrusion, justifying the approximation used to

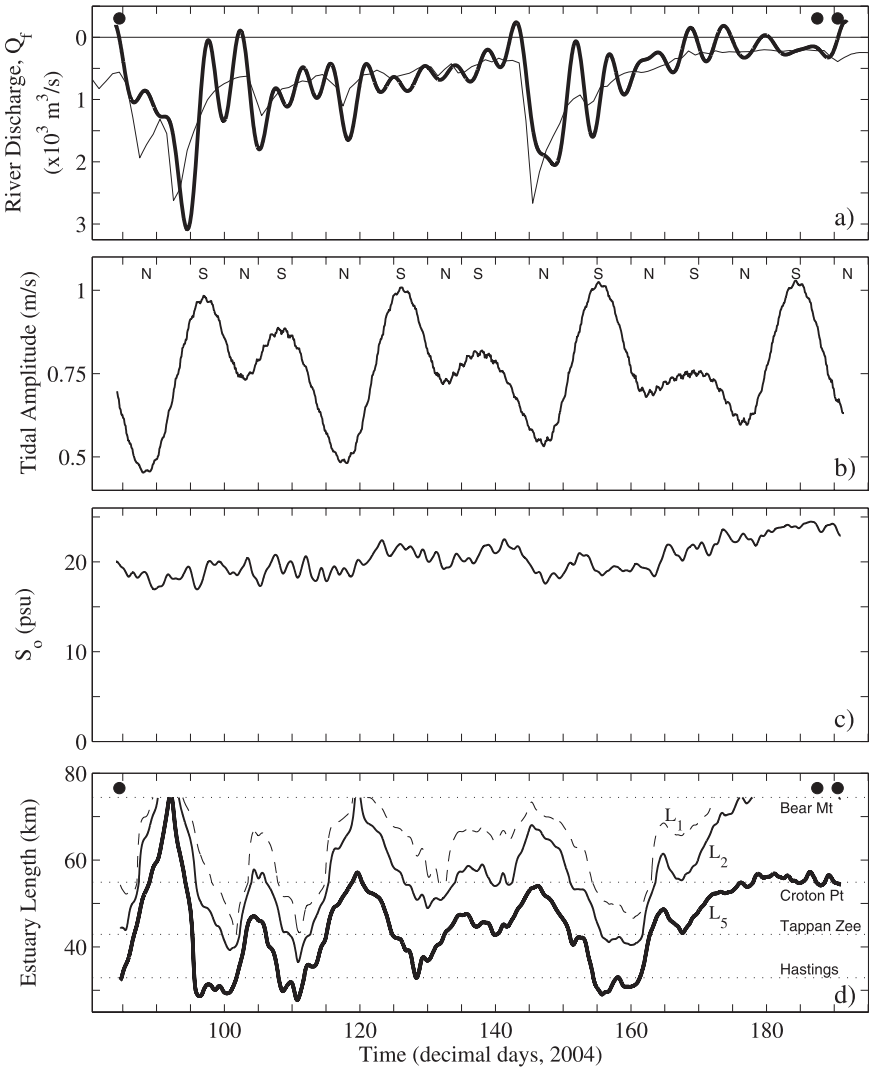

FIG. 4. (a) River discharge Q_f vs time estimated from ADCPs (thick line) and obtained from the USGS Green Island stream gauge No. 01358000 (scaled by a factor of 1.6 to account for watershed oceanward of the gauge; thin line). Data from the USGS stream gauge, located upstream of the Troy Dam, do not contain the synoptic (~2–5 day) discharge variability apparent in the records from the ADCPs located within the estuary and with direct connection to the open ocean (Lerczak et al. 2006). (b) Tidal amplitude. The letters N and S indicate the times of neap and spring tidal conditions, respectively. (c) Subtidal, top, and bottom average salinity at the Battery (Fig. 1) S_o. (d) Distance along the river from the Battery to the location of the 5- (L_5), 2- (L_2), and 1-psu (L_1) vertically averaged salinity. Locations of selected moorings are indicated by horizontal dotted lines. Filled circles at the top of (a) and (d) indicate the times of the hydrographic surveys shown in Fig. 6.

relate the along-estuary salinity gradient to L in the derivation of the response model (Fig. 2). The largest deviations from the linear, self-similar salinity intrusion occur during high discharge ($Q_f > 1000$ m^3 s^{-1}).

During the period of high discharge (before day 160), the response of L_5 to spring–neap variations in tidal amplitude was large. For example, L_5 ranged from 27 to >75 km (Fig. 4d). The most dramatic variation occurred during the first storm event (day 94), which was centered on a transition from apogean neap to spring tide. Here L_5 was >75 km at day 92.0, 3.6 days after a neap tide and when freshwater discharge was increasing, and shortened to 28 km in about 4 days. For the first six neap tides, there was a corresponding peak in L_5. All peaks in L_5 lagged the neap tide minimum (average lag = 1.8 days, standard deviation = 1.5 days), with the exception

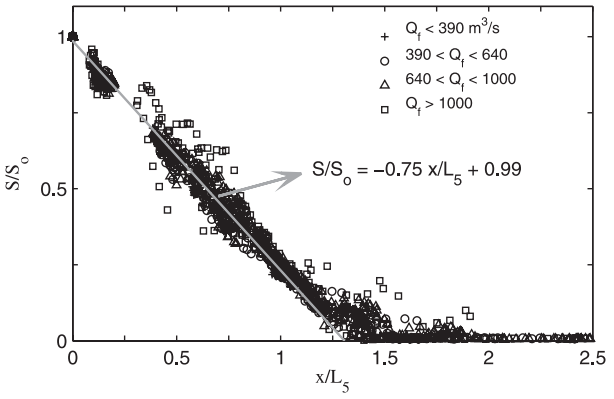

FIG. 5. Vertically averaged salinity S scaled by S_o vs along-estuary distance x scaled by L_5 from the 2004 field study. Different symbols correspond to different freshwater discharge ranges. The gray line is a linear fit using data with $x/L_5 < 1.25$.

of the fifth peak, which preceded the corresponding neap tide by 1.1 days. During the period of low river discharge (after day 165), the response of L_5 to the spring–neap cycle was negligible and the length approached a time-independent value of about 56 km.

Along-estuary salinity sections from hydrographic surveys at the beginning and end of the study period are shown in Fig. 6. Individual casts from each survey were first advected up or down estuary, using vertically averaged currents from the ADCP time series, to minimize the effect of tidal advection during the period of a survey and to bring the casts from each survey to a common time within the tidal cycle (the midpoint of a tidal excursion, that is, either maximum flood or maximum ebb). This processing minimizes the variability due to tidal advection, which can shift the salinity intrusion up and down estuary by as much as 15 km.

At the beginning of the study period (Fig. 6a), during the spring-to-neap transition, stratification was strong and the estuary was relatively short. The section was taken during a period of high and increasing Q_f. Two hydrographic sections from the end of the study period (Figs. 6b,c) were taken three days apart, with one centered on and the other toward the end of the spring-to-neap transition. While the stratification clearly increased over this period, the length of the estuary did not change significantly.

b. Long-term U.S. Geological Survey data

To study the time response of estuary length over a longer time period and a broader range of conditions than those observed during the 2004 field study, we use long-term time series of near-surface salinity, river discharge, and tidal current amplitude. Daily average near-surface salinity time series were collected in the Hudson by the U.S. Geological Survey (USGS) at Hastings, West Point, and Poughkeepsie (stations 1376304, 1374019, and 1372058 and 33, 84, and 120 river km north of the Battery, respectively; Fig. 1). Freshwater discharge time series at Green Island Dam (about 250 river km north of the Battery at station 01358000) were also obtained from the USGS. This discharge data was multiplied by a factor of 1.6 to account for the fraction of the Hudson River watershed south of the dam (Lerczak et al. 2006). While this time series accurately describes the variations in discharge due to snowmelt and rain events, it does not contain the meteorological band (2–4 day) variations in discharge, mainly caused by offshore sea level forcing and wind events (Fig. 4; Lerczak et al. 2006; Ralston et al. 2008). Finally, a record of the spring–neap variations in tidal velocity amplitude U_T was obtained using the National Oceanic and Atmospheric Administration (NOAA) tidal harmonic predictions at the George Washington Bridge and Haverstraw (Fig. 1). A continuous record, 13.4 yr in length (May 1992 to October 2005), was analyzed using the combined time series.

To estimate L_5 over the entire record, we first estimate vertically averaged subtidal salinity S at the Battery and Hastings based on variations in USGS near-surface salinity at Hastings S_{sH}. Variations in stratification due to variations in mixing and buoyancy forcing, which influence the relationship between S_{sH} and S, must be taken into account. Based on regressions between S estimated from the 2004 data and the long-term time series, we find that the simplest model that explains most of the variance in S is

$$S_l = a_l + b_l S_{sH} + c_l Q_f + d_l U_T' + e_l U_T'^2, \qquad (12)$$

where the subscript l refers to either the Battery or Hastings. Coefficients (a_l, b_l, etc.) were determined by least squares estimation using the 2004 time series of S at the Battery and Hastings separately for four different discharge ranges. The estimate based on Eq. (12) explains 91% and 90% of the variance in S at the Battery and Hastings, respectively (Fig. 7). For periods of very high discharge, S_{sH} often had a value of zero and could not be used reliably to estimate S. Thus we ignore periods when $Q_f > 2500$ m^3 s^{-1}, and extreme discharge events are not considered in subsequent analyses. Vertically averaged subtidal salinity at West Point and Poughkeepsie were assumed to be well represented by the USGS near-surface time series, which ranged from 0 to 9.4 and 0 to 1.0 psu at the two locations, respectively.

Similar to the 2004 data, L_5 for the long-term record was estimated by linearly interpolating salinities between the four along-estuary locations. The long-term

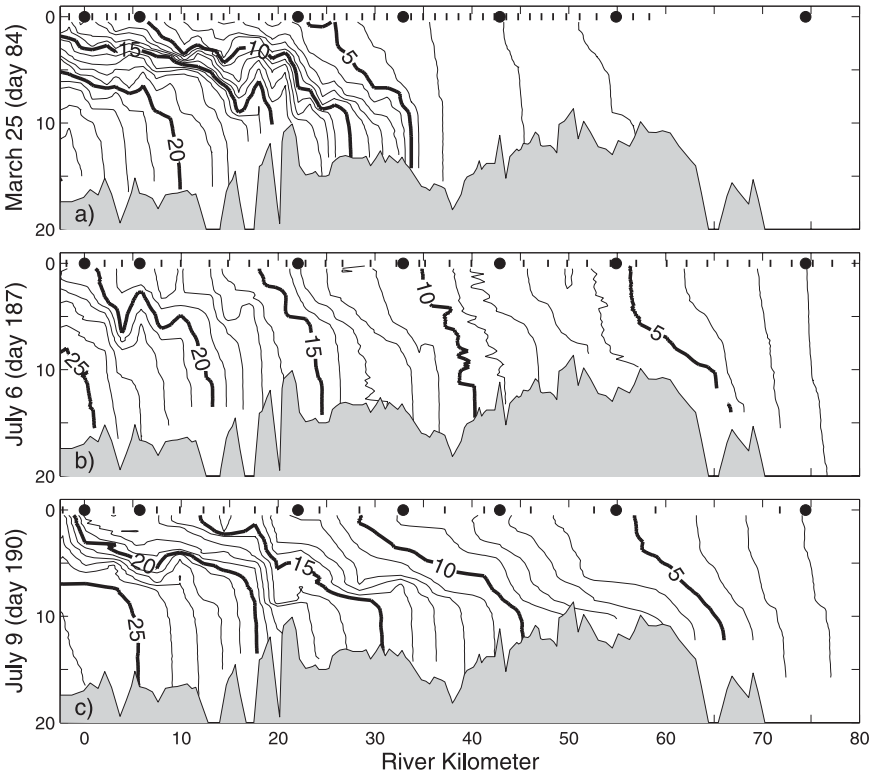

FIG. 6. Along-estuary sections of salinity obtained from hydrographic surveys conducted on (a) 25 Mar, (b) 6 Jul, and (c) 9 Jul 2004. Individual casts from each survey were first advected up or down estuary, using vertically averaged currents from the ADCP time series, in order to minimize the effect of tidal advection during the period of a survey and to bring the casts from each survey to a common time within the tidal cycle (the midpoint of a tidal excursion, i.e., either maximum flood or maximum ebb). The contour interval is 1 psu. Short vertical lines at the top of each panel indicate locations of CTD casts after being advected to a common time within a tidal cycle. Filled circles indicate mooring locations.

estimate of L_5 is well correlated with the 2004 estimate (Fig. 8, inset). However, the long-term estimate of estuary length was systematically about 5–10 km longer than the estimate from the 2004 study, which will be made apparent in the analysis of the scaling of estuary length with freshwater discharge (section 6b). This is likely due to the poorer resolution of the along-estuary structure of S in the long-term dataset (four along-estuary locations) compared to the 2004 dataset (seven locations).

Variations in the long-term estimate of L_5 are consistent with those in the 2004 estimate. Estuary length was negatively correlated with Q_f (Figs. 8 and 9a). Typically, maximum discharge occurred during the winter and spring months, when L_5 was smallest. During summer months with extended periods of low discharge, L_5 slowly increased and typically approached a steady value. High-frequency variations in L_5 were largest during periods of high discharge. For example, within the spring–neap frequency band (periods between 12 and 30 days), variations in L_5 increased in amplitude by a factor of 4 from low to high discharge (Fig. 9b).

4. Fit of data to linear response model

The freshwater discharge and tidal amplitude vary on multiple time scales, so we solve (7) by first computing its Fourier transform:

$$-i\omega\tilde{L}' + \frac{1}{\tau}\tilde{L}' = -\frac{L_o}{\tau}\tilde{f},$$

$$\tilde{L}' = -L_o\tilde{f}(1 - i\omega\tau)^{-1}, \tag{13}$$

where a tilde indicates Fourier transformed variables. The solution to (13) is

$$\hat{L} = L_o\left(1 + \int_{-\infty}^{\infty}\tilde{f}\frac{e^{-i\omega t}}{1 - i\omega\tau}d\omega\right) + \Delta e^{-t/\tau}, \tag{14}$$

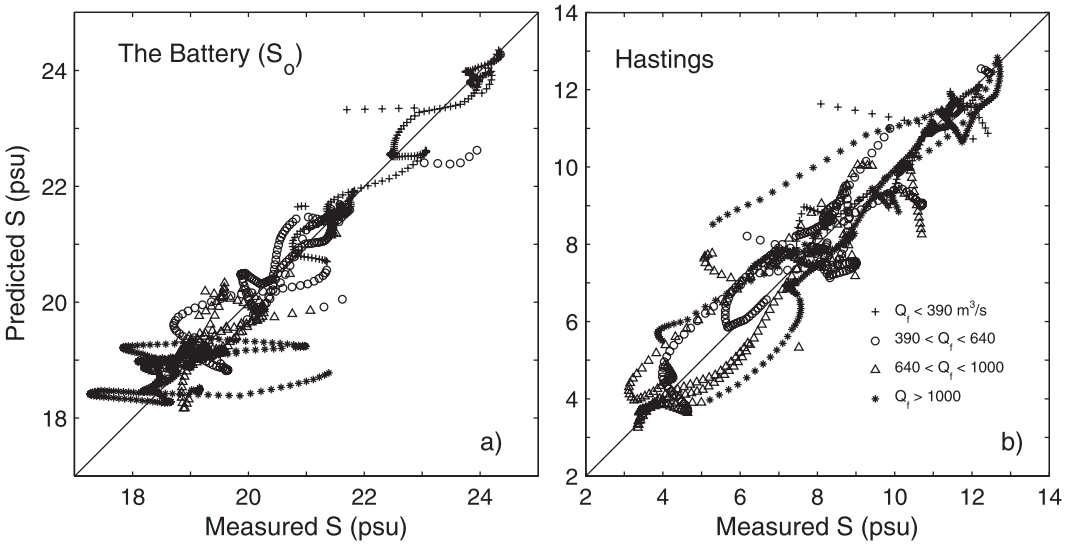

FIG. 7. Predicted vertically averaged subtidal salinity S using Eq. (12) and least squares estimated coefficients at (a) the Battery and (b) Hastings vs S estimated from surface and bottom salinity time series during the 2004 field study. Coefficients were estimated separately for four different freshwater discharge ranges (indicated by different symbols in the panels).

where $\hat{L}$ refers to the estimate of the estuarine length from the linear response model. The last term in (14) is the homogeneous solution and Δ is a transient length that decays over the response time scale. For the purpose of comparing the model to the observed length of the Hudson estuary and to test the theoretical dependence of τ and L_o on Q_o, we leave τ, L_o, and Δ as free parameters and do not impose the values predicted by the salt balance equation as expressed in (9) and (10).

We chose to compare L_5 to the response model, because it remained within the spatial limits of the mooring array for the entire deployment period of the 2004 study, with the exception of a 9-h period on day 92 when it passed the up-estuary limit of the array (Fig. 4d). For this brief period, L_5 was assigned a value of 74 km (the location of the northernmost mooring). The three free parameters L_o, τ, and Δ were estimated by minimizing the mean-squared deviations between the model and the data:

$$\Gamma = \frac{1}{N}\sum[\hat{L}(L_o, \tau, \Delta) - L_5]^2, \qquad (15)$$

where the sum is over the time series used in the fit.

5. Derived response parameters

The sensitivity of the estuarine response time and equilibrium estuarine length to river discharge was determined by fitting L_5 to the model, using both forcing functions f_1 and f_2, for periods of time with different mean discharges Q_o. Four different time periods in 2004 were considered: the entire study period; the nearly constant, high discharge period between days 113 and 135; the low discharge period at the end of the record between days 165 and 191; and the first storm between days 84 and 113. Deviations of the tidal amplitude were calculated relative to the tidal amplitude averaged over the entire study period U_{To}. Results of the fits are summarized in Table 1 and Fig. 10.

a. Eddy viscosity proportional to tidal amplitude

We first describe results for the model with eddy viscosity proportional to tidal amplitude (forcing function f_1). When the entire record is used in the fit, the model response time is estimated to be 7.7 days and the response amplitude for spring–neap variations in tidal forcing is 29% the maximal response. Spring–neap variations in estuarine length are apparent in the fit. However, the fit fails to capture the large spring–neap response in L_5 during high discharge at the beginning of the record (before day 160) and overpredicts the spring–neap response during low discharge (after day 160; Fig. 10c).

Skill is improved when periods of high and low Q_o are fit separately, as made apparent by the reduction in the mean-squared deviation between $\hat{L}$ and L_5 for the high and low Q_o periods in comparison to the fit of the entire record (Fig. 10c and relative skill column in Table 1). For the high and low flow periods, Γ is reduced by 76%

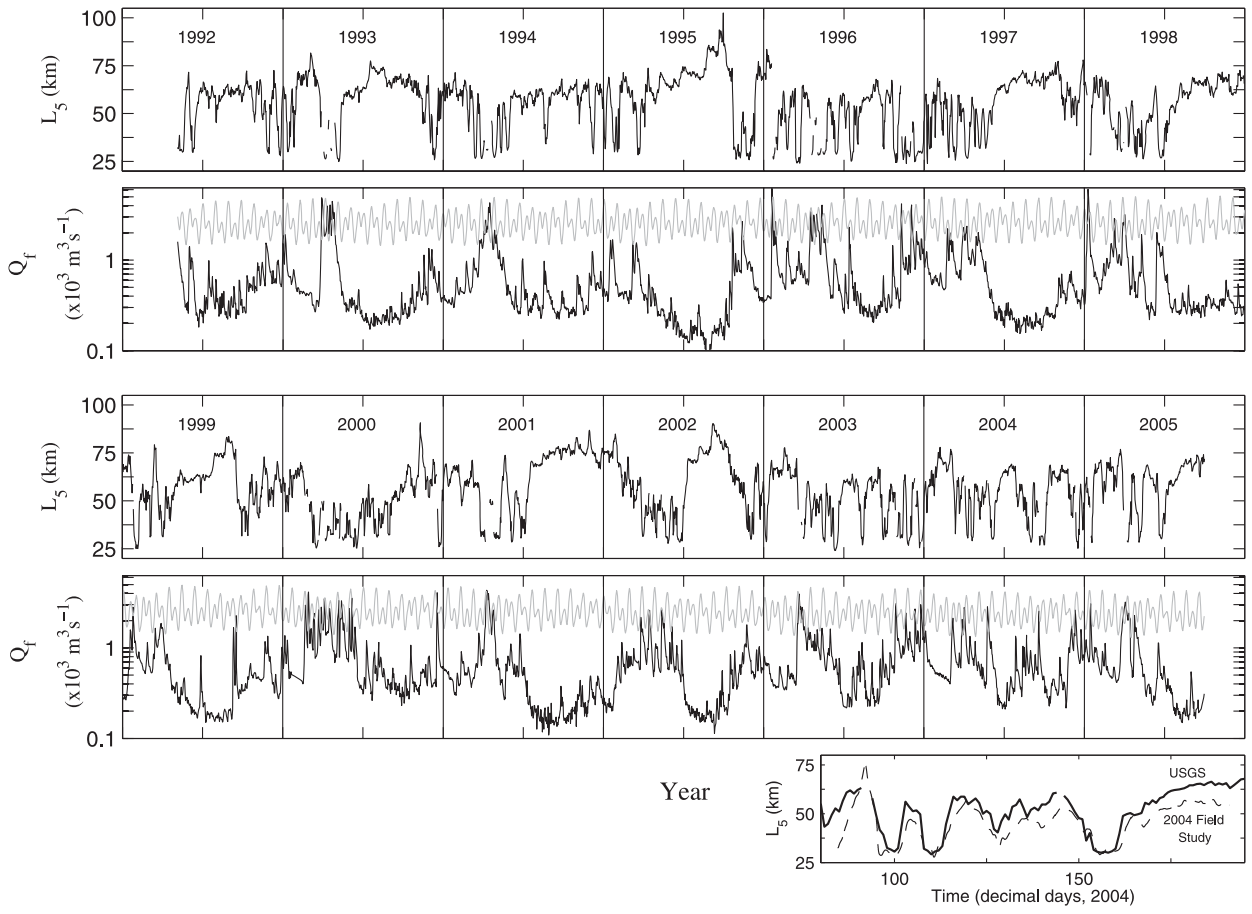

FIG. 8. Estimated L_5, freshwater discharge Q_f, and tidal current amplitude U_T, over the long-term (13.4 yr) time period. Here Q_f is plotted on a log scale; U_T (gray line), plotted on a linear scale, is an average of the NOAA tidal predictions at the George Washington Bridge and Haverstraw and has a range of 0.6–1.2 m s^{-1}. Values of L_5 are not plotted when $Q_f > 2500$ m^3 s^{-1}. The inset compares L_5 estimated from the long-term USGS time series (solid line) with that from the 2004 field study (dashed line).

and 87%, respectively. For the initial storm period, the model is unable to reproduce the large spring–neap variations in estuarine length that are apparent in the observations, and the reduction in Γ is only 13%.

Significant differences in the estuarine response are apparent. During the high discharge period, τ_1 is estimated to be 3.3 days, whereas τ_1 is estimated to be an order of magnitude longer (35.9 days) for the low Q_o period. The amplitude of the response to spring–neap variations in forcing is significantly larger for the high Q_o period (58% maximal response) in comparison to the low period Q_o (6% maximal response).

b. Stratification-dependent eddy viscosity

There are slight differences in L_o and τ between the fits with the eddy diffusivity proportional to U_T and those with stratification-dependent diffusivity (forcing function f_2; Table 1). However, relative changes in these parameters for different fitting periods are similar. The model with stratification-dependent diffusivity has a higher skill at predicting L_5, except for the low flow period, where both models have high skill (90% of the variance in L_5 is explained by the model with both forcing functions).

c. Model fits to running time blocks of data

To more precisely assess the dependence of model parameters on Q_o and to test the theoretical scalings in (9) and (10), we calculated model fits using time blocks of data 22 days in length (roughly 1.5 spring–neap cycles) using the 2004 data. Fits of this type were made from the beginning to the end of the study period, with successive time blocks incremented by 1.5 days from the previous time block. Model parameters and skill are summarized in Fig. 11. Variations in L_o, τ, and Δ are similar for the two models considered, and only parameters for the model with stratification-dependent diffusivity (using f_2) are shown in Fig. 11. Running fits

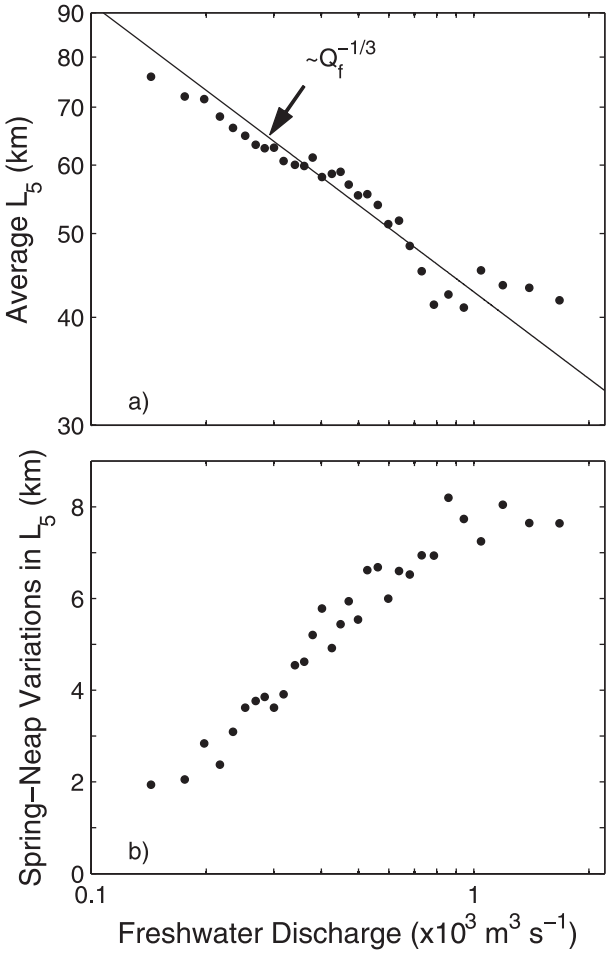

FIG. 9. (a) Bin-average L_5 vs binned freshwater discharge Q_f from the long-term (13.4 yr) dataset. (b) Standard deviation of spring–neap variations (bandpassed between periods of 12 and 30 days) in L_5 vs Q_f. The range of each discharge bin was chosen to have a uniform number of data points (150 days or about 10 spring–neap cycles) within each bin.

were also calculated using the long-term data and are discussed in the next section.

The response time is slightly lower during the period of the first storm (before day 113; $\bar{\tau}_2 = 3.0$ days, standard deviation = 0.3 days) compared to the high discharge period between the storms (days 113–135; $\bar{\tau}_2 = 4.6$ days, standard deviation = 1.2 days). During a minimum in Q_o centered on day 134 and prior to the second storm, L_{o2} and τ_2 reached local maximum values before returning to low values during the high discharge period of the second storm (days 147–156; $\bar{\tau}_2 = 3.4$ days, standard deviation = 0.1 days; $L_{o2} = 41.0$ km, standard deviation = 0.6 km). During the low flow period after day 165, τ_2 and L_{o2} increased to their largest values over the entire time series. During this period, the estimated response time scale is longer than the time block used in the model fits. Here, the model is essentially fitting the time scale of the apparent exponential relaxation of L_5 to a steady value of 56 km after day 165 (Figs. 4d and 10c).

Large spring–neap variations are apparent in the transient amplitude Δ_2 (Fig. 11e) because the tidal and discharge forcing is not stationary; that is, the spectral content of the forcing for one 22-day block of time is different from the next block of time. The linear model must adjust to the local forcing of a particular time block. The only way the linear model allows for this is through the transient homogeneous solution.

During the period of high discharge, the model with stratification-dependent eddy diffusivity had a higher level of skill in fitting to L_5 in comparison to the model with eddy diffusivity proportional to U_T (Fig. 11f). During the low discharge period, both models fit the data with comparable levels of skill.

6. Discussion

The response of the length of the Hudson estuary is significantly different during periods of high river discharge compared to periods of low discharge. When discharge is high, large spring–neap fluctuations in estuary length occur, with the estuary being longest typically 1.5–4 days after neap tide. When discharge is low, the estuary responds very little over a spring–neap cycle. These observations are consistent with the observational studies of Bowen and Geyer (2003) and Lerczak et al. (2006) and the modeling studies of MacCready (2007), Ralston et al. (2008), and Warner et al. (2005), who observed large spring–neap variations in the estuary length and the landward salt flux during moderate-to-high discharge conditions and weak response of the total estuary salt content to spring–neap tidal variations during low flow conditions.

a. Response time

During periods of high discharge, the response time is shorter than the spring–neap period, resulting in large spring–neap variations in estuary length. During periods of low discharge, the response time is considerably longer than the spring–neap period, resulting in a weak response. These order of magnitude variations in τ from high to low discharge are consistent with the modeling study of MacCready (2007). The dependence of estimated τ on Q_o is consistent with the response time varying linearly with the time it takes a water parcel, traveling at the speed of the freshwater discharge, to traverse the length of the estuary (Figs. 12a,b). However, the modeled response time is about 3–4 times larger than the theoretical linear

TABLE 1. Parameters from least squares fits of estuary length L_5 to linear response model expressed in Eq. (7). The subscript 1 refers to fits to the model with diffusivity proportional to tidal amplitude. The subscript 2 refers to fits to the model with a stratification-dependent diffusivity.

	Period (days)	Q_o ($m^3\ s^{-1}$)	std dev(Q_f)/Q_o	L_{o1}/L_{o2} (km)	τ_1/τ_2 (days)	Δ_1/Δ_2 (km)	φ_1/φ_2 (days)[a]	Amp_1/Amp_2[b]	$Skill_1/Skill_2$[c]	Relative skill[d]
Full record	106	690	0.88	45.7/45.9	7.7/5.8	−3.4/−6.5	3.0/2.8	0.29/0.38	0.65/0.71	0/0
High flow	22	750	0.40	45.9/45.4	3.3/4.2	−10.5/−8.6	2.2/2.5	0.58/0.49	0.88/0.94	0.76/0.46
Low flow	26	170	1.0	67.2/70.7	35.9/40.4	−18.1/−21.3	3.5/3.6	0.06/0.06	0.90/0.90	0.87/0.96
First storm	29	1100	0.64	43.3/43.7	3.8/3.1	−7.6/−14.0	2.4/2.2	0.53/0.60	0.61/0.77	0.13/0.22

[a] The estimated phase lag is for forcing oscillating at the spring–neap period (T_f = 14.8 days).
[b] The response amplitude $(1 + \omega^2\tau^2)^{-1/2}$ is estimated for forcing that oscillates at T_f.
[c] Skill is defined as the fraction of the variance of L_5 explained by the model fit $1 - \Sigma(\hat{L} - L_5)^2/\Sigma(L_5 - \bar{L}_5)^2$, where $\hat{L}$ is the model fit and $\bar{L}_5$ is the time average of L_5 over the period that is being fit to the model.
[d] Relative skill is a measure of the improvement of a fit for a specified time period in comparison to the model prediction for that period using model parameters from the fit of the full record ($\hat{L}_{all}$) $1 - \Sigma(\hat{L} - L_5)^2/\Sigma(\hat{L}_{all} - L_5)^2$, where the sums are over the specified time period.

response times expressed in Eqs. (10). Response times that are several times larger than theoretical predictions have also been reported for simulations of idealized, partially stratified estuaries (Hetland and Geyer 2004) and for the Hudson estuary model of MacCready (2007).

Several reasons may explain this discrepancy. First, in the expression for the along-estuary dispersion rate, Eq.

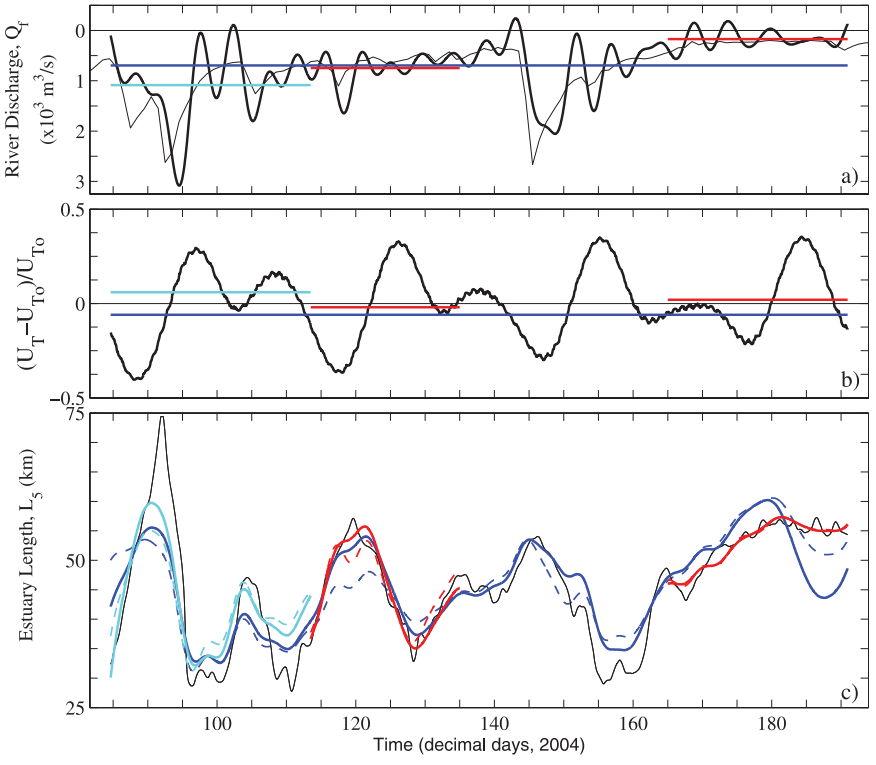

FIG. 10. Forcing functions and model fits of L_5 using the 2004 data. (a) River discharge vs time. Colored horizontal lines indicate the time periods over which the linear response model was fit to the data. The vertical level of these lines indicates the average discharge Q_o for that period. (b) Tidal amplitude forcing function. Colored horizontal lines (staggered vertically) indicate the time periods over which the linear response model was fit to the data. (c) Estuary length L_5 (black line). Colored lines indicate the linear response model fit for the different time periods using a vertical eddy diffusivity that is proportional to tidal amplitude (dashed lines) and a stratification-dependent eddy diffusivity (solid lines).

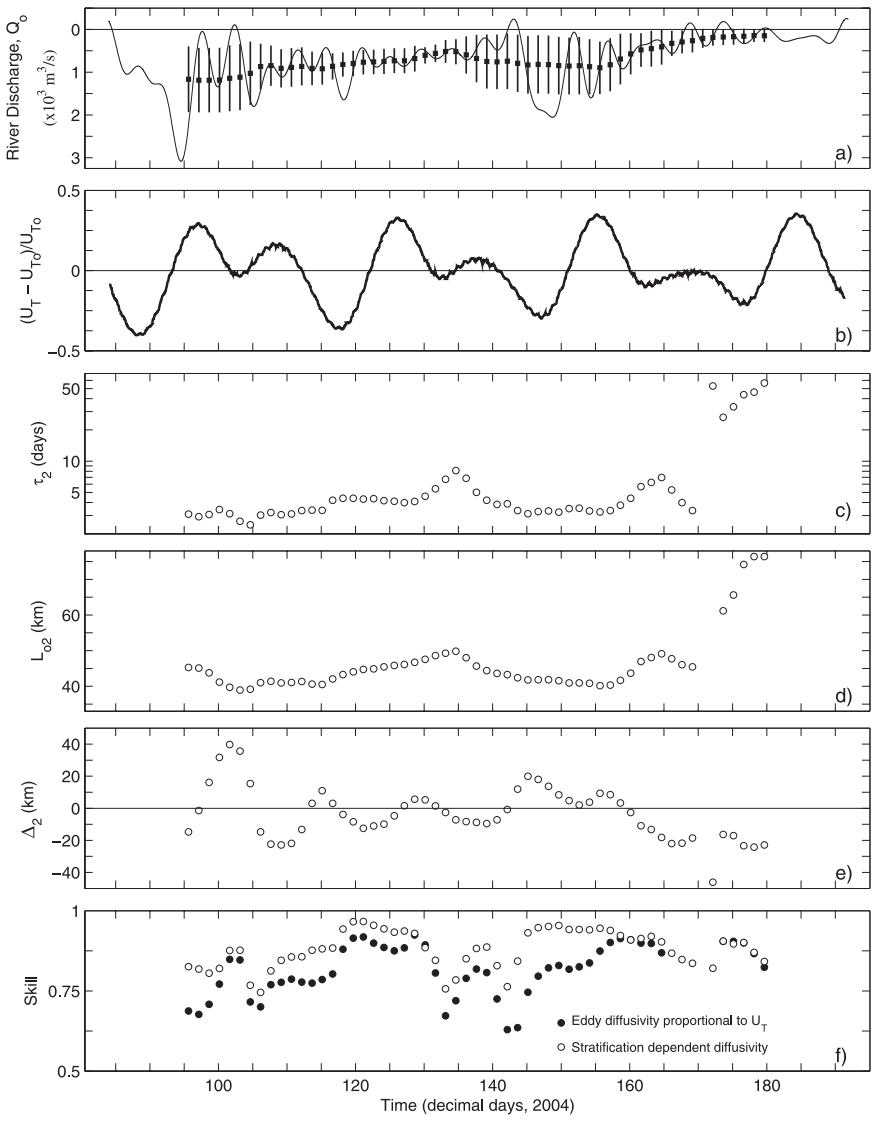

FIG. 11. Linear response parameters for model fits to 22-day-long periods calculated over the entire 2004 study period, with each successive time block incremented by 1.5 days from the previous time block. Parameters are indicated by circles centered on the time block used in the fit. (a) Mean discharge (Q_o, filled squares). Thin line shows the observed discharge Q_f. Vertical lines indicate ± 1 standard deviation of Q_f over the fitting period. (b) Tidal amplitude deviations relative to mean tidal amplitude. (c) Fitted response time τ_2 for model with stratification-dependent eddy diffusivity. (d) Equilibrium estuarine length L_{o2}. (e) Transient length Δ_2. (f) Model skill defined as the fraction of the variance of L_5 explained by the model fit $1 - \Sigma(\hat{L} - L_5)^2/\Sigma(L_5 - \bar{L}_5)^2$, where $\hat{L}$ is the model fit and $\bar{L}_5$ is the average of L_5 over the 22-day period being fit to the model.

(2), it is assumed that the exchange circulation and stratification that drive the up-estuary salt flux spinup instantaneously. However, the spinup time for the exchange circulation and stratification is finite and may be comparable to or longer than the theoretically predicted response time. For example, a minimum time scale $T_{\Delta S}$ for the spinup of stratification during a spring-to-neap transition is the time it takes the stratification to be generated by the straining of the longitudinal salinity gradient by the estuarine exchange flow: $T_{\Delta S} = (\Delta S/S_o)(L_o/\Delta u)$, where ΔS is the top-to-bottom salinity difference during neap tide and Δu is the amplitude of the exchange circulation. Using reasonable values for moderate-to-high discharge conditions ($\Delta S = 10$ psu, $S_o = 20$ psu, $L_o = 50$ km, and $\Delta u = 0.1$ m s^{-1}), $T_{\Delta S}$ is 3 days. This is a minimum spinup time scale because it

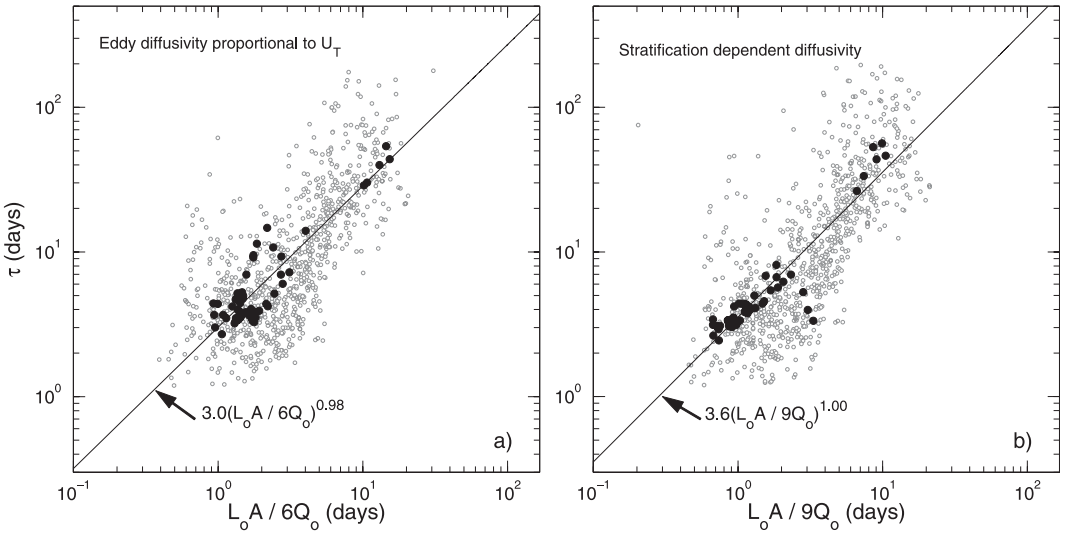

FIG. 12. Fitted response time τ vs theoretical response time from Eqs. (10) for (a) the model with eddy diffusivity proportional to U_T and (b) the model with stratification-dependent diffusivity. Filled circles are for values of τ, L_o, and Q_o obtained from the model fits of 22-day-long blocks of data using the 2004 data (see Fig. 11). Open circles are from the long-term dataset. The cross-sectional area A is taken to be 1.5×10^4 m^2. The line is a linear least squares fit to the 2004 data.

ignores the competing destruction of stratification by vertical mixing of salt. This time scale may be considerably longer for low discharge periods, when buoyancy forcing and exchange circulation are relatively weak and the estuary is relatively long (weak longitudinal salinity gradient). However, this would not explain the long response times, compared to theoretical predictions, of MacCready (2007), whose model also assumes instantaneous spinup of exchange circulation and stratification.

Second, the nonlinearity of the salt balance [Eqs. (1) and (2)] may act to slow the adjustment of the estuary. Hetland and Geyer (2004) show that, for an idealized partially stratified estuary in a uniform channel, while the steady-state length, stratification, and exchange flow follow the theoretical scalings of Hansen and Rattray (1965) and Chatwin (1976), the response time to step changes in Q_f is longer than the theoretically predicted linear response and is dependent on whether the change is from high to low discharge or low to high discharge. They hypothesize that the asymmetry in response is due to quadratic bottom drag. However, the inconsistency with linear theory may be due to the nonlinearity in the dynamics and the factor-of-5 step change in discharge they impose.

Finally, while studies have demonstrated that the up-estuary salt flux in the Hudson is dominated by subtidal vertical shear dispersion (Bowen and Geyer 2003; Lerczak et al. 2006), the model of Hansen and Rattray (1965) for a constant depth and uniform channel, from which the dispersion rate used here is derived, is not likely to fully capture the physics of vertical mixing and estuary exchange in the Hudson, with both longitudinal and lateral variations in bathymetry. Ralston et al. (2008), for example, have shown that longitudinal variations in bathymetry—in particular, the geometric factor in the expression for equilibrium length (Eq. 9), $G \equiv (AH^5)^{1/3}$—can influence the scaling of estuary length with discharge, particularly in estuaries with significant longitudinal bathymetric variations, such as northern San Francisco Bay. Geometric variations are also likely to influence the response time.

b. Scaling of L_o with Q_o

The equilibrium length L_o is an estimate of the steady length of the estuary for average tidal amplitude. In this analysis, L_o scales with ${Q_o}^{-\delta}$, where δ is estimated to be nearly the same for the two mixing schemes considered here (Figs. 9a and 13a,b). For the 2004 data, least squares estimates of δ are 0.29 and 0.27 for forcing functions f_1 and f_2, respectively. While estimates of L_o for a particular Q_o are 5–10 km longer for the long-term data compared to the 2004 data, the scalings are similar ($\delta = 0.32$ and 0.33 for f_1 and f_2, respectively, using the long-term data). The estimates of δ are closer to the theoretical prediction for the model with eddy diffusivity proportional to U_T ($\delta = 1/3$) than for the model with the stratification-dependent diffusivity ($\delta = 2/9$). However, scatter in the data does not allow either of the models to be obviously rejected.

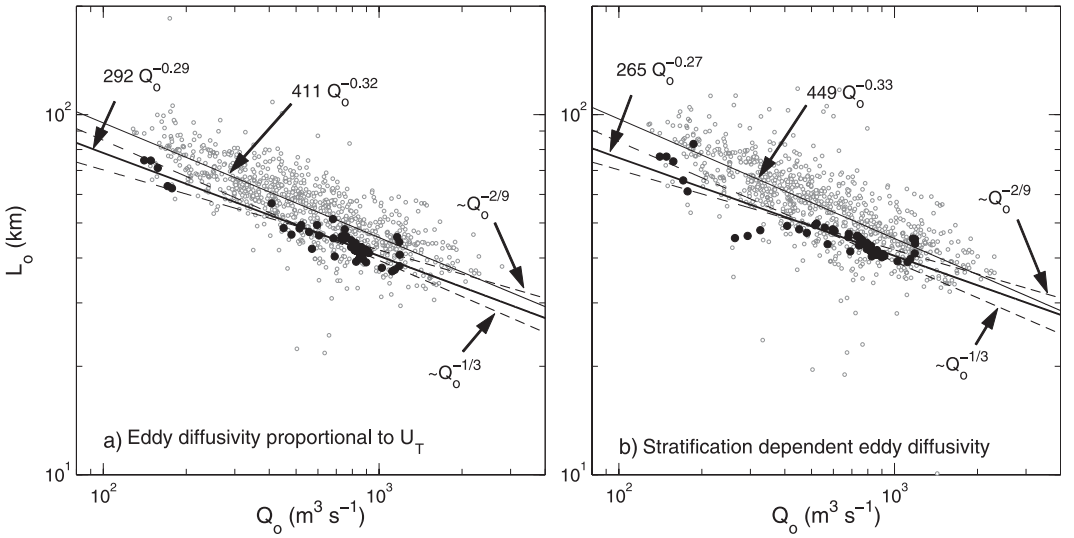

FIG. 13. Fitted equilibrium estuarine length L_o vs mean freshwater discharge Q_o. Filled circles are from the model fits of 22-day-long blocks of data from the 2004 study (see Fig. 11) using (a) the model with eddy diffusivity proportional to U_T and (b) the model with a stratification-dependent eddy diffusivity. Open circles are from the long-term dataset. The solid thick line is a linear least squares fit to the 2004 data. The solid thin line is a linear least squares fit to the long-term (13.4 yr) dataset. The dashed lines indicate the theoretical scalings for an exchange-dominated estuary expressed in Eqs. (9).

This analysis is consistent with the observations of the Hudson estuary length by Abood (1974) for Q_o less than 1000 $m^3\ s^{-1}$, as well as the modeling of Ralston et al. (2008). The analysis of Abood (1974) suggests that for higher mean discharges, which are not resolved well in this study, the dependence of L_o on Q_o is stronger. A stronger sensitivity of L_o at high Q_o would be expected if the estuary behaves as a two-layer salt wedge, with hydraulics being the principle physics controlling the length of the estuary. For example, Keulegan (1966) predicts that the length of an arrested salt wedge should scale with $Q_o^{-2.5}$. Hetland and Geyer (2004) also show that the sensitivity of the length of an idealized partially stratified estuary to Q_o increases for high discharge, when the estuary has the structure of an arrested salt wedge.

c. Model performance

Based on the modeled response, the equilibrium Hudson estuary length and its variation over a spring–neap cycle versus Q_o are summarized in Fig. 14. For low Q_o, the estuary length changes very little over a spring–neap cycle and is far from equilibrium for instantaneous tidal conditions; that is, the tendency term is the dominant term on the left side of Eq. (7) and the estuary cannot respond fast enough to approach the quasi-steady length for spring or neap tidal conditions (dashed lines in Fig. 14). For high Q_o, the changes in estuary length over the spring–neap cycle approach the quasi-steady limit. However, even in this limit, time dependence is important and the two terms on the left side of Eq. (7) are comparable in magnitude ($\omega\tau \approx 1$).

A failure of the model is its underprediction of the large amplitude spring–neap variations in estuary length during periods of high discharge. This is particularly apparent for the fit over the period of the first storm (Table 1 and cyan lines in Fig. 10), where the model is unable to capture the large increase in L_5 that peaks on day 92. This discrepancy highlights an inadequacy of this linear model to completely represent the variations of a fundamentally nonlinear estuarine system. In the linear model, response phase and amplitude to sinusoidal forcing are dependent on the single parameter ($\omega\tau$; Fig. 3) and maximum response occurs when the phase difference between the response and the forcing is zero. In the fit to the period of the first storm, the model is unable to reconcile the observed large amplitude response with the significant phase lag of this response (3.6 days or 85°).

The model of Ralston et al. (2008), which solves the nonlinear salt balance Eq. (1) and the Hansen and Rattray (1965) and Chatwin (1976) formulation for the longitudinal dispersion rate [Eq. (2)], also fails to capture the large variations in the salinity intrusion when mixing is weak and discharge is moderate to high and the estuary begins to behave like a salt wedge, with a sharp pycnocline and nearly fresh surface waters and nearly oceanic bottom waters.

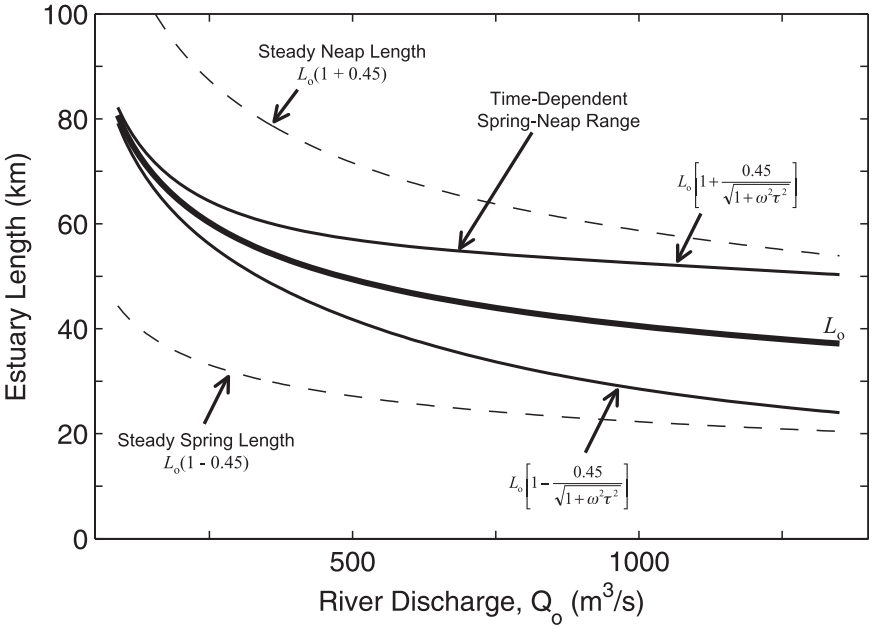

FIG. 14. Equilibrium estuarine length vs river discharge. Thick line indicates the predicted steady length for average tidal forcing L_o from the fit in Fig. 13b. Thin lines indicate the spring–neap cycle range in estuary length, where ω is the frequency of the spring–neap cycle and the factor of 0.45 is the approximate amplitude of the spring–neap forcing function (Figs. 10b and 11b). The response time is calculated from the fits in Figs. 12b and 13b. Dashed lines indicate the steady length for steady spring and neap tide conditions, that is, the time-independent length that the estuary would achieve for a time-independent spring or neap tidal amplitude at the specified river discharge.

While this analysis does not allow either of the scalings in Eq. (9) to be rejected, it is clear that the model with forcing function f_2, using a stratification-dependent diffusivity, predicts L_5 with higher skill than the model with forcing function f_1, using a diffusivity proportional to U_T. This is particularly true during periods of moderate-to-high discharge. The principle reasons for this are that f_2 has a higher forcing amplitude [prefactor outside of brackets in Eq. (8)] compared to f_1 and emphasizes variations in tidal amplitude relative to variations in discharge. Ralston et al. (2008) also show highest skill when the stratification-dependent eddy diffusivity and viscosity are used in their model.

d. Generalization of linear response model

In the formulation of the salt balance presented above, the linear response and equilibrium length of the estuary is determined by the dependence of the along-estuary salt dispersion rate K on the external parameters U_T and Q_f and the internal parameter dS/dx. For a dispersion rate with the general form

$$K = K_o\left(\frac{U_T}{U_{To}}\right)^{\alpha}\left(\frac{L_o}{S_o}\frac{dS}{dx}\right)^{\beta}\left(\frac{Q_f}{Q_o}\right)^{\gamma}, \qquad (16)$$

where K_o is the dispersion rate for mean values of parameters, the linear response model is given by

$$\frac{dL'}{dt} + \frac{1}{\tau}L' = \frac{L_o}{\tau}\left[\left(\frac{\gamma-1}{\beta+1}\right)\frac{Q'}{Q_o} + \left(\frac{\alpha}{\beta+1}\right)\frac{U_T'}{U_{To}}\right], \quad (17)$$

$$L_o \propto U_{To}^{\frac{\alpha}{\beta+1}} Q_o^{\frac{\gamma-1}{\beta+1}}, \quad \text{and} \qquad (18)$$

$$\tau = \frac{1}{2(\beta+1)}\frac{L_o A}{Q_o}. \qquad (19)$$

For the model with eddy diffusivity proportional to U_T, the scales α, β, γ are -3, 2, 0. For the stratification-dependent diffusivity, they are -6, 7/2, 0. Several authors report on the dependence of equilibrium length and response time on α, β, γ. For example, Kranenburg (1986) shows that τ decreases with increasing β, consistent with Eq. (19). MacCready (2007) studies the response time and the dependence of L_o on Q_f for a dispersion rate that is dominated by estuarine exchange (the model considered here, with eddy diffusivity proportional to U_T) and a dispersion rate dominated by stirring by horizontal, tidally driven eddies (see below).

Monismith et al. (2002) argue that vertical mixing decreases with increased discharge, because of increasing

stratification with increasing discharge, resulting in a discharge-dependent dispersion rate ($\gamma > 0$). They suggest that this can explain the very weak dependence of the length of the northern San Francisco Bay estuary on river discharge ($L_o \propto Q_o^{-1/7}$) compared to the scaling based on exchange-dominated salt flux of Hansen and Rattray (1965) [L_{o1}; Eq. (9)]. In contrast, Ralston et al. (2008) argue that, if mixing has a strong discharge dependence, then the length of the Hudson estuary should also exhibit a weak discharge dependence similar to northern San Francisco Bay. They suggest that differences in bathymetry explain the differences in the responses of the two estuaries to changes in discharge.

Finally, for estuaries with up-estuary salt fluxes that are driven by mechanisms other than subtidal steady shear dispersion due to the exchange circulation, different linear responses are expected. For example, in estuaries where dispersion is driven by horizontal tidal eddies ($K = c_o B U_T$, where c_o is a constant and B is the width of the estuary; Banas et al. 2004; MacCready 2007), $(\alpha, \beta, \gamma) = (1, 0, 0)$. The response time is predicted to be 3 times slower than that of an exchange-dominated estuary. More importantly, the dependence of L_o on Q_o is markedly different, with $L_o \propto U_T^1 Q_o^{-1}$.

7. Summary

The linear response model presented here provides an objective framework for studying the response of an estuary to changes in forcing and for separating the equilibrium estuary length L_o for mean discharge and mean tidal amplitude, from variations in length due to variations in forcing. However, it must be emphasized that the salt conservation Eq. (1) from which it is derived is nonlinear and assumes a uniform channel. This puts the validity of the model in question during periods when the variations in forcing are as big as or bigger than the mean forcing and for estuaries with large bathymetric variations. The river discharge, which can vary by over an order of magnitude, poses the biggest challenge to the linearization. Nonetheless, if applied to other estuaries for which dispersion is dominated by mechanisms other than subtidal vertical shear dispersion, it can provide insight into the response of the estuary under different forcing regimes as well as aid in identifying the mechanisms that drive dispersion.

Acknowledgments. This study was generously funded by Hudson River Foundation Grant 005/03A and NSF Grant OCE-0452054. Lerczak also received partial support from the Woods Hole Center for Oceans and Human Health, NSF Grant OCE-0430724 and NIEHS Grant 1-P50-ES012742-01.

REFERENCES

Abood, K. A., 1974: Circulation in the Hudson River estuary. *Hudson River Colloquium,* Vol. 250, O. A. Roels, Ed., New York Academy of Sciences, 38–111.

Banas, N. S., B. M. Hickey, P. MacCready, and J. A. Newton, 2004: Dynamics of Willapa Bay, Washington: A highly unsteady partially mixed estuary. *J. Phys. Oceanogr.,* **34,** 2413–2427.

Bowen, M. M., and W. R. Geyer, 2003: Salt transport and the time-dependent salt balance of a partially stratified estuary. *J. Geophys. Res.,* **108,** 3158, doi:10.1029/2001JC001231.

Chatwin, P. C., 1976: Some remarks on the maintenance of the salinity distribution in estuaries. *Estuarine Coastal Mar. Sci.,* **4,** 555–566.

Geyer, W. R., and R. Chant, 2006: The physical oceanography processes in the Hudson River estuary. *The Hudson River Estuary,* J. S. Levinton and J. R. Waldman, Eds., Cambridge University Press, 13–23.

——, J. H. Trowbridge, and M. M. Bowen, 2000: The dynamics of a partially mixed estuary. *J. Phys. Oceanogr.,* **30,** 2035–2048.

Hansen, D. V., and M. Rattray Jr., 1965: Gravitational circulation in straits and estuaries. *J. Mar. Res.,* **23,** 104–122.

Harleman, D. R. F., and M. L. Thatcher, 1974: Longitudinal dispersion and unsteady salinity intrusion in estuaries. *Houille Blanche,* **1/2,** 25–33.

Hetland, R. D., and W. R. Geyer, 2004: An idealized study of the structure of long, partially mixed estuaries. *J. Phys. Oceanogr.,* **34,** 2677–2691.

Hunkins, K., 1981: Salt dispersion in the Hudson estuary. *J. Phys. Oceanogr.,* **11,** 729–738.

Kranenburg, C., 1986: A time scale for long-term salt intrusion in well-mixed estuaries. *J. Phys. Oceanogr.,* **16,** 1329–1331.

Keulegan, G. H., 1966: The mechanism of an arrested salt wedge. *Estuary and Coastline Hydrodynamics,* A. T. Ippen, Ed., McGraw-Hill, 546–574.

Lerczak, J. A., W. R. Geyer, and R. J. Chant, 2006: Mechanisms driving the time-dependent salt flux in a partially stratified estuary. *J. Phys. Oceanogr.,* **36,** 2296–2311.

MacCready, P., 2007: Estuarine adjustment. *J. Phys. Oceanogr.,* **37,** 2133–2145.

Monismith, S. G., W. Kimmerer, J. R. Burau, and M. T. Stacey, 2002: Structure and flow-induced variability of the subtidal salinity field in northern San Francisco Bay. *J. Phys. Oceanogr.,* **32,** 3003–3019.

Ralston, D. K., W. R. Geyer, and J. A. Lerczak, 2008: Subtidal salinity and velocity in the Hudson River estuary: Observations and modeling. *J. Phys. Oceanogr.,* **38,** 753–770.

Simpson, J. H., R. Vennell, and A. J. Souza, 2001: The salt fluxes in a tidally-energetic estuary. *Estuarine Coastal Shelf Sci.,* **52,** 131–142.

Smith, R., 1996: Combined effects of buoyancy and tides upon longitudinal dispersion. *Buoyancy Effects on Coastal and Estuarine Dynamics,* D. G. Aubrey and C. T. Friedrichs, Eds., Amer. Geophys. Union, 319–329.

Stacey, M. T., and D. K. Ralston, 2005: The scaling and structure of the estuarine bottom boundary layer. *J. Phys. Oceanogr.,* **35,** 55–71.

——, J. R. Burau, and S. G. Monismith, 2001: The creation of residual flows in a partially stratified estuary. *J. Geophys. Res.,* **106,** 17 013–17 038.

Vallino, J. J., and C. S. Hopkinson, 1998: Estimation of dispersion and characteristic mixing times in Plum Island Sound estuary. *Estuarine Coastal Shelf Sci.,* **46,** 333–350.

Warner, J. C., W. R. Geyer, and J. A. Lerczak, 2005: Numerical modeling of an estuary: A comprehensive skill assessment. *J. Geophys. Res.,* **110,** C05001, doi:10.1029/2004JC002691.

Wells, A. W., and J. R. Young, 1992: Long-term variability and predictability of Hudson River physical and chemical characteristics. *Estuarine Research in the 1980s,* C. L. Smith, Ed., State University of New York Press, 29–58.